

Vocke, Timo and Johanning, Bernd

Studies on a mulcher by field test and simulation

In the research project „Optimization of energy input at rest-stubble processing“ supported by the European Fund of Regional Development the central connection between used energy and the achieved level of treatment is examined. By detecting the drive power of a mulching machine at different operating conditions it is possible to represent the various power components. Using the model of a subsystem and the evaluation of measurement results of a field trial it could be projected on the deflection behaviour of the tools.

Keywords

Field test, stubble processing, simulation

Abstract

Landtechnik 67 (2012), no. 4, pp. 251–255, 6 figures, 4 references

■ The increasing cultivation of energy crops is leading to ever tighter crop rotations in practical farming. A frequent problem encountered in this connection is the inadequate rotting of the residual stubble remaining on the field after harvesting. This stubble offers a habitat for pests and fusarium fungi that infect the follower crop [1]. This results in harvest losses and massive use of pesticides and insecticides. The mechanical treatment of the stubble, in other words cutting off close to ground level and destroying the culm structure at the same time, allows fast rotting of the stubble. This minimizes the risk of pests and fusarium fungi and it is generally then possible to do without the use of chemical agents to treat the residual stubble.

This study examines the connection between the energy input and the level of treatment on the one hand via a classic field trial and on the other hand via laboratory experiments with individual culms. The field trials are conducted primarily

on areas used for silage and grain maize cultivation with commercially available flail mulchers. The average power requirement ascertained here together with the degree of treatment achieved is defined as the present state of the art and serves as a benchmark for the following development within the scope of the project.

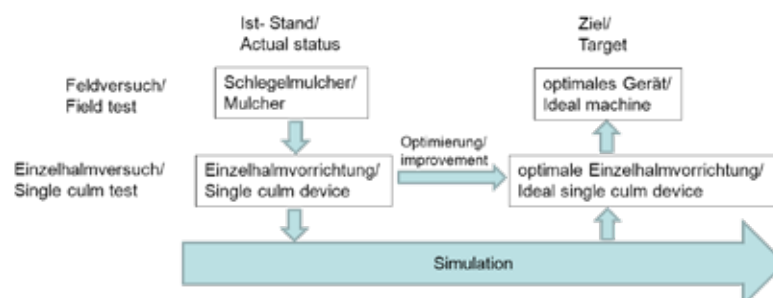
Parallel with this the results of the field trials are transferred to the individual culm experiments in the laboratory. The energy input and level of treatment are first optimized in further individual culm experiments, the results of which are then verified in the field trial (**Figure 1**).

In order to obtain a statement about the quality of treatment it is planned to infect samples from the field and laboratory experiments with bacteria that occur in cultivated fields. The subsequent observation and evaluation of the rotting process provides information about the effect of the preceding treatment. This makes it possible to establish the relationship between cause and effect

Overall system and operating mode of the flail mulcher

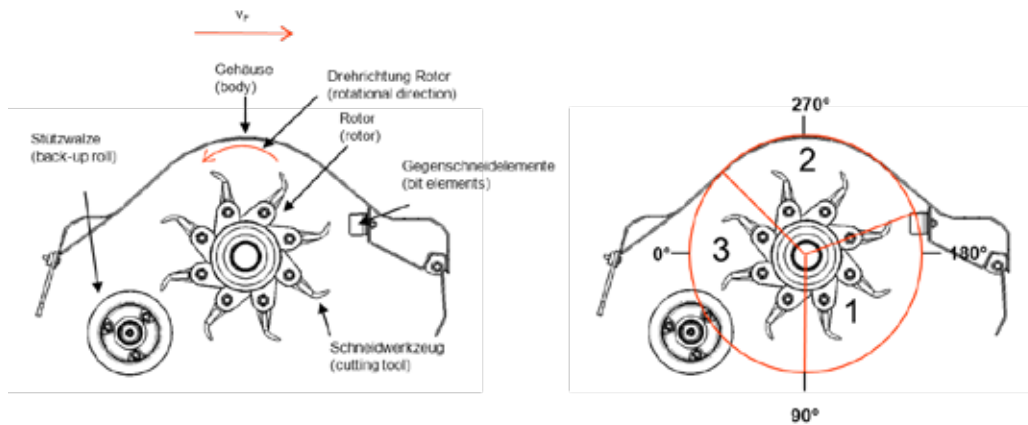
The machine used most frequently to treat residual stubble nowadays is the flail mulcher. **Figure 2** shows the schematic assembly of such an implement.

Fig. 1



Experimental strategy for process optimization

Fig. 2



Schematic assembly and operating mode of a mulcher

The working cycle of a tool mounted on the rotor can be divided into three zones as regards the operating mode:

■ **Zone 1:** The stubble material is cut off close to ground level and conveyed into the closed mulcher body. Here it accumulates and is shredded through frequent chopping by the bit elements. It is often possible to fit additional bit elements inside the bodies to boost treatment intensity. The components used are pure congesting elements with which no chopping using bit elements, such as takes place for example in combine harvesters or forage harvesters, is achieved. The rated speed of the rotors ($n_{Rot, rat}$) lies in the range of 25 1/s, so that with corresponding dimensions tool speeds (v_{tool}) ≤ 65 m/s result.

■ **Zone 2:** In this zone the material is conveyed along the body. Given appropriate material parameters (moisture content, ripeness, throughput rate) post-mulching is possible on the grounds of the mass inertia of the stubble material and the friction at the body. For treating grain maize fields, this means that there can be up to nine metric tons of harvest residues on the ground per hectare that can then be mulched with a mean dry matter content of approx. 40 % [2]. At the end of this zone the mulched material leaves the turning circle of the tools tangentially and is flung to the ground between the body and the back-up roller.

■ **Zone 3:** The rotor and the tools only displace air here. The power requirement in this zone thus corresponds to pure idling performance.

Field tests

Figure 3 shows results of the first series of tests, carried out chiefly on grain maize fields in autumn 2011.

The chart shows the specific mean idling ($P_{spez,Y}$) and drive power inputs in working mode for the toolless rotor and two different cutting tools. These are two common tools used to treat residual stubble – the multiple-element Y-blade and the hammer flail. The specific total input power of the respective tool is calculated as follows:

$$P_{spez,H} = P_{Rot, leer} + P_{H, leer} + P_{H, Nutz} \quad \text{bzw.}$$

$$P_{spez,Y} = P_{Rot, leer} + P_{Y, leer} + P_{Y, Nutz} \quad (\text{Eq. 1})$$

The idling power $P_{Rot, idle}$ is made up of the mechanical friction losses in the drive train, the bearing condition and the flow resistance of the rotor without tools. The quantities $P_{H, idle}$ and $P_{Y, idle}$ only contain the tool-specific idling powers occurring at rated speed. The working input power $P_{H, work}$ and $P_{Y, work}$ are made up of a number of components – cutting, chopping and conveying at a working speed of 4 km/h.

Different total power inputs occur under identical conditions of use, resulting primarily from the different idling powers.

Breakdown of the mean torque over a working cycle

To obtain a more detailed analysis a method used to examine cutting processes in the field of mowers [3] has been adapted to study flail mulchers. In a first step the mean torque acting on the rotor per tool is calculated and divided between the three zones (**Figure 1**). It is necessary to take the losses in the drive train into account here. This is possible with the aid of measurements of the toolless rotor (**Figure 2**). In this way the mean driving torque levels at the rotor per tool unit $M_{H4, mean}$ and $M_{Y4, mean}$, are obtained, (**Figure 4**).

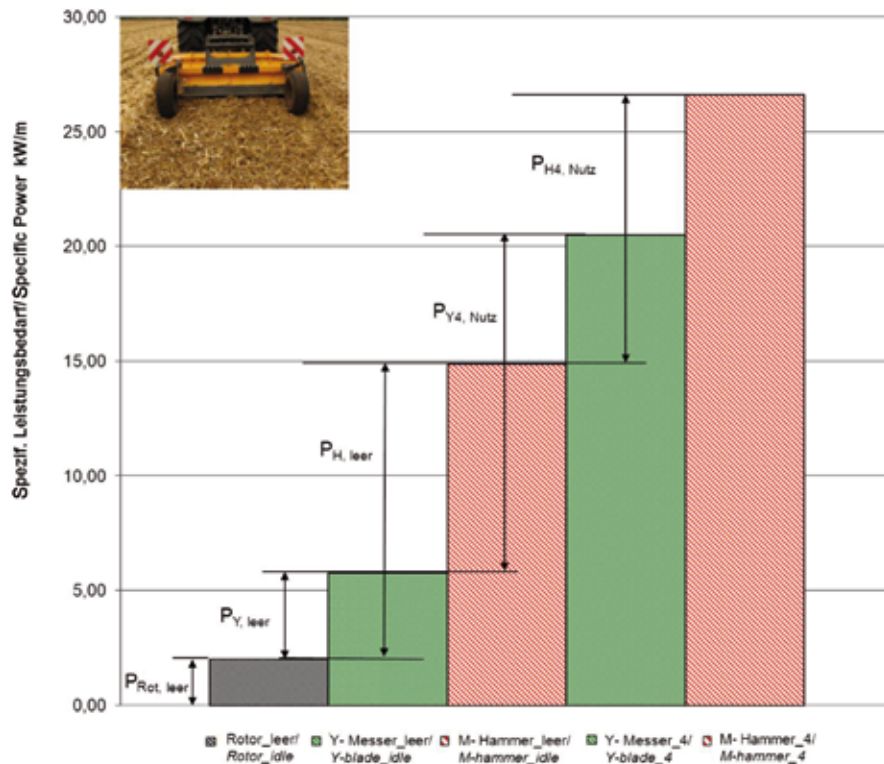
For the rotor input power to be identical between measurement and the curve by work zone after passing through a working cycle, the areas of the respective torque curves included after a cycle must be equally large (equation 2).

$$\int_0^{360^\circ} M_{H4, mittel} d\varphi_R = \int_0^{360^\circ} M_{H4, Zyklus} d\varphi_R \quad \text{bzw.}$$

$$\int_0^{360^\circ} M_{Y4, mittel} d\varphi_R = \int_0^{360^\circ} M_{Y4, Zyklus} d\varphi_R \quad (\text{Eq. 2})$$

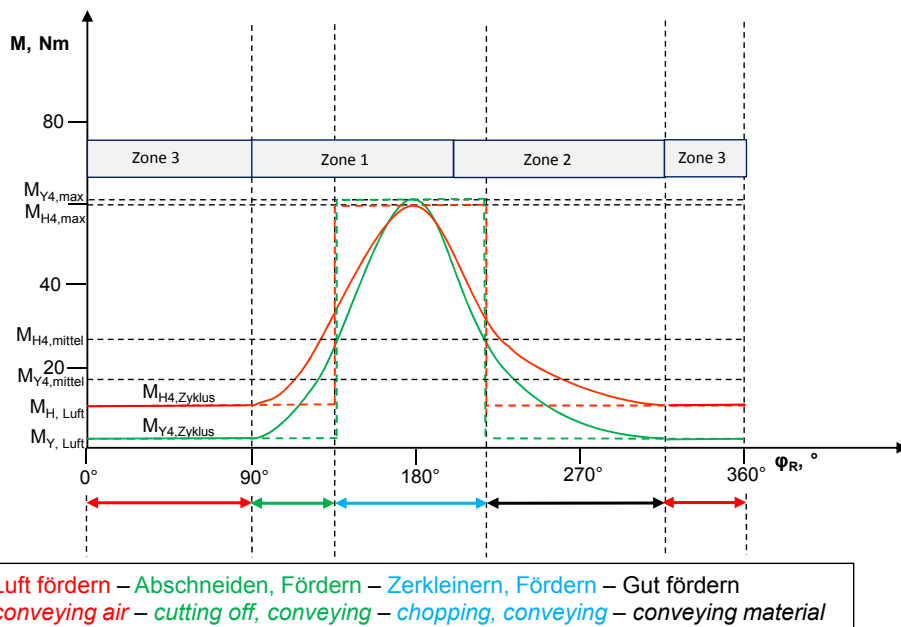
Here φ_R describes the actual angle of the rotor (**Figure 2**). The range of pure air conveying (zone 3) can be read off directly

Fig. 3



Total input power in idle and working mode

Fig. 4

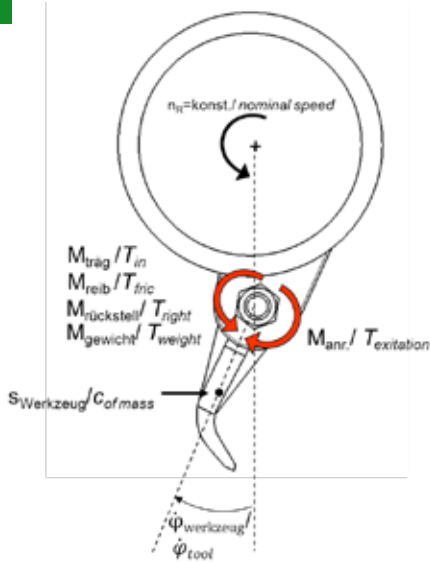


Total input power in idle and working mode

from the measurements in **Figure 2** and be converted to the acting torque per tool at the rotor. $M_{H, \text{air}}$ and $M_{Y, \text{air}}$ at 12.4 Nm and 3.5 Nm are distinctly below the mean measured torques $M_{H4, \text{mean}} = 24.8$ Nm and $M_{Y4, \text{mean}} = 18.3$ Nm. A comparison of the numerical values shows clearly that this division is expedient for considering a working cycle.

In order to develop the most detailed possible breakdown from the model, zone 1 was subdivided into two ranges. In the range from 90° - approx. 135° material is primarily cut off, while in the range of the bit element, 135° - 215° , the material congests and is chopped more intensively with multiple cuts. Initially it is only the torque in this range that is raised in the form

Fig. 5



Part system „rotor- tool“

of a rectangular signal resulting from the mathematical breakdown of the mean torques by the three zones. The dotted lines result with the calculated maximum torques $M_{H4, \max} = 62 \text{ Nm}$ and $M_{Y4, \max} = 62.7 \text{ Nm}$ (Figure 4).

A comparison of the tool-specific curves reveals that the maximum torque of the Y-blade is somewhat higher than that of the hammer tools, although the mean torque measured is lower. The substantially lower aerodynamic resistance of the Y-blades is critical here.

By analogy with Kammerer [4], a real torque curve during a cycle was estimated qualitatively by the parabolas drawn in.

Mean tool deflections in idling and working modes

As regards the individual culm experiments, the overall system “mulcher” under review here was reduced to a subsystem “rotor-flail” to produce a simulation model in Matlab/Simulink.

For the modelling it is assumed in simplified terms that the rotor speed n_R remains constant. Figure 5 shows the torques acting on the fastening point during the positively accelerated deflection. By simulating this subsystem it is possible, for instance, to determine the mean tool deflection that is very difficult to measure on the machine in working mode. Consideration of the mean deflection with pendulum-type mounting of the tools in working mode indirectly provides information about the power range in which the machine is operating. If the performance limit is exceeded, the tools fold away and no work is performed.

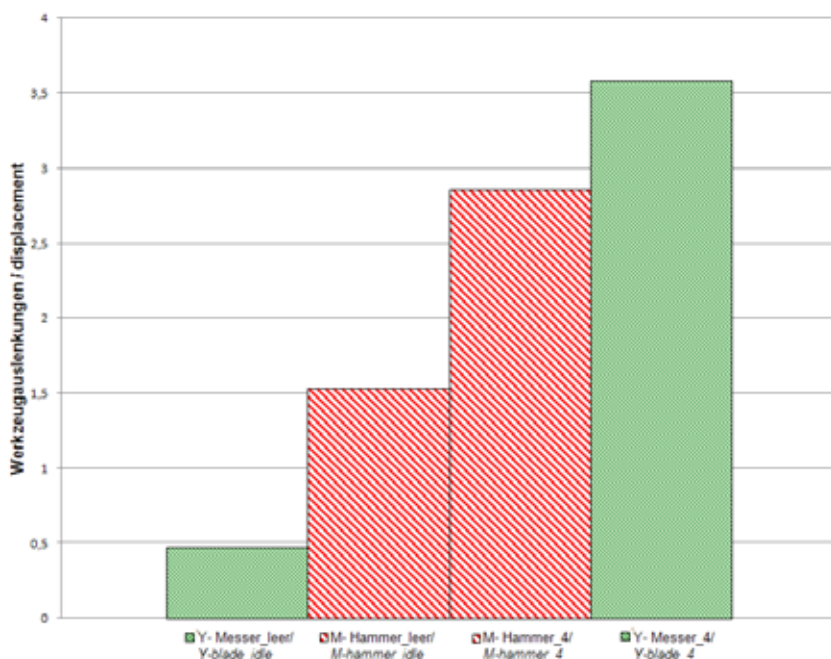
Application of the simulation with the curves shown in Figure 4 results in the mean tool deflections set out in Figure 6.

Both tools only deflect slightly in idling operation at 0.4° and 1.6° respectively. The somewhat larger deflection of the hammer tool despite the greater weight, which is responsible for higher friction and restoring torques, is due to the substantially higher aerodynamic resistance of the hammer flail (Figure 3). In conjunction with these plate-shaped tools the mulcher develops the function of a blower.

In working mode on the other hand, the Y-blade deflects further when activated with the calculated maximum torque, as the potential necessary for transmitting the cutting forces is only achieved here.

Mean deflection angles of several degrees in working mode or even folding away on contact with obstacles, as is the case with mowers [2], is not conceivable for flail mulchers with a tool weight of 3 kg, taking these first results into account.

Fig. 6



Middle tool displacement while idle- and working mode

Conclusions

With the test arrangement from the field trial the total power can be divided into three power constituents. On closer consideration, however, the rotor power $P_{\text{Rot, idle}}$ and the working powers $P_{\text{Y4, work}}$ and $P_{\text{H4, work}}$ are made up of further individual power components. To optimize the system under energy aspects it is expedient to examine in particular the composition of the working power in order to influence the power requirement.

The idling powers $P_{\text{H, idle}}$ and $P_{\text{Y, idle}}$ on the other hand are only influenced by the tool geometry and can be captured clearly. Their shares in the total input power are high due to the high aerodynamic resistance and optimizing could help to reduce the energy input.

It is clear from considering the input powers that the energy input can be optimized by reducing the aerodynamic resistance of the tools, as well as via the actual working processes (cutting, chopping, conveying).

Furthermore, the division into three zones allows provisional breakdown of the power input during a working cycle, i.e. one rotor revolution. In combination with the simulation model of the “rotor-flail” subsystem, the mean tool deflections in idling and working modes can be shown. The slight deflections indicate that the mulcher still possesses substantial power reserves at the operating point examined.

The initial results of the research project make it clear that the classic field trial is not sufficient to identify and determine the cutting and chopping powers precisely. Consequently further results can only be achieved via series of experiments on the individual culm test rig with supporting simulation.

Literature

- [1] Zellner, M. (2009): Der Maiszünsler in Bayern. Fachvortrag, Bayerische Landesanstalt für Landwirtschaft, Institut für Pflanzenschutz, http://www.lfl.bayern.de/ips/blattfruechte_mais/25671/linkurl_0_2.pdf, Zugriff am 10.05.2012
- [2] Hammerschmid, W.; Handler, F. (1992): Vergleichsuntersuchung von Schlegelhäckslern. Forschungsbericht Nr. 33, BLT Wieselburg
- [3] Horstmann, J. (1998): Untersuchungen zur Reduzierung von Antriebschäden im Getriebe eines Scheibenmäherwerkes bei Hinderniskontakt. Dissertation, Technische Universität Braunschweig, VDI Fortschritt-Berichte, Reihe 14, Nr. 90, VDI-Verlag, Düsseldorf
- [4] Kämmerer, D. (2002): Der Schneid- und Fördervorgang im Mähdescherhäckslern. Dissertation, Technische Universität Braunschweig

Authors

Dipl.-Ing. (FH) Timo Vocke, M.Sc. is research officer at the Labor für Landtechnik und mobile Arbeitsmaschinen at Hochschule Osnabrück (Director **Prof. Dr.-Ing. B. Johanning**), Albrechtstrasse 30, 49009 Osnabrück, e-mail: T.Vocke@hs-osnabrueck.de

Additional information

ERDF research project (European Regional Development Fund).